

Investigation of the Replication Quality of Microstructures on Injection Moulded Specimens Made from Recycled Polypropylene Composites Reinforced with Carbon Nanotubes

Krisztián Kun¹, Attila Bata¹, Ferenc Ronkay^{1*}

¹ Department of Innovative Vehicles and Materials, GAMF Faculty Engineering and Computer Science, John von Neumann University, H-6000 Kecskemét, Izsáki st. 10., Hungary

* Corresponding author, e-mail: ronkay.ferenc@nje.hu

Received: 07 May 2024, Accepted: 15 July 2024, Published online: 22 July 2024

Abstract

During the research, functional microstructures were created on the cavity surface of the injection moulding tool using femtosecond laser technology. Automotive-grade polypropylene (PP), as well as its recycled and carbon nanotube-reinforced composites, were used as the raw materials. The replicated structures were examined using confocal microscopy. It is expected that by optimizing the process parameters, the filling of the structured cavity surface with nanocomposite materials can reach a quality level comparable to plastic specimens made from non-reinforced raw materials. The aim is to provide results of scientific and industrial value to demonstrate the influence of the modified mould surface on the flow of the polymer melt and thus on the filling of the injection moulded products.

Keywords

carbon nanotubes, recycling, microstructure, replication, end-of-life vehicles

1 Introduction

The global automotive plastics market was valued at USD 29.50 billion in 2022. It is expected to grow at a compound annual growth rate (CAGR) of 5% between 2023 and 2030. A low- to mid-range passenger car comprises 6% to 10% plastics, with a total weight of over 110–120 kg. Reducing vehicle weight and drawing increased attention to emission control are key factors to boost the growth of the high-performance plastics market. In terms of manufacturing technology, injection moulding accounted for the largest share of over 56% of all processes in 2022, yet in terms of raw material processed, polypropylene (PP) and its recycled version led the automotive plastics market with a 32% share [1]. Designers use simulation software to increase the inertia of parts in key directions at the design stage by using ribs, which are surface features that are considered in the macro-region. The definition of microstructure is also used in polymer technology according to the standard [2, 3], B. Sha et al. referred to microstructures as surface area units below 200 μm in their study [4]. These structures, in addition to serving aesthetic purposes, modify the mechanical properties of the product. In this case,

the design of the micro-ribs (microstructures) can have a specific strength-enhancing effect due to geometrical (inertia) and material structural changes (filling process) [5–7].

Theilade and Hansen found that temperature is an important factor in replication, as increasing the temperature of the melt nearly doubled the filling of microstructures [8]. A similar change in height is observed when the injection rate is increased. Sha et al. also studied the replication of micro geometry and observed the formation of so-called rings in PP base material, which they explained by the material "hesitating", i.e. temporarily stopping and filling the micro-surface only after reaching the final cavity pressure [4]. Zhang et al. reported [9] that the MFI of unfilled base material decreased drastically with adding 5 w/w% CNT, but further increasing the ratio of the reinforcing agent did not modify the MFI. This phenomenon has been confirmed by Attia et al. [10] in their research that was conducted on low-viscosity materials. They reported that high mould temperatures can reduce the thickness of the solidified layer and delay the cooling of the cavity, allowing more material to enter the structures. The term has been used to describe the effect

where low-viscosity fluid enters the structured die cavity at high velocity and then bypasses and "flows over" the microstructures. This effect can be more significant in the presence of a reinforcing phase, which influences the viscosity of the material. The connection between the filling of the microstructures and the CNT reinforcing phase is less discussed in the literature [11–14].

In line with the development trends in the automotive industry, PP and its recycled and reinforced versions were investigated as raw materials. Numerous scientific studies have shown that CNT reinforcement results in a degradation of the flow properties of polymers [15–17] and that the quality of the mould surface has an additional significant effect on the filling of the mould cavity and the cooling efficiency [18–22]. With the growth of nano-reinforced polymer composites, the relationship between processing parameters, reinforcement content and the filling of micro-ribs formed on the tool surface has become an increasingly important area of research [23–29].

The present research aims to study the relationship between the femtosecond laser-treated cavity of the injection mould and the melt containing the reinforcing (CNT) phase. The goal is to investigate the relationship between the surface micro-ribs (functional microstructures) and different processing parameters (Fig. 1).

2 Materials and methods

2.1 Materials

The original PP co-polymer raw material used is the Tipplen K499 block co-polymer produced by MOL Petrochemicals. It is applied in the automotive industry to make interior supports, coolants, window washer tanks and battery housings. The carbon nanotubes used are Plasticyl PP2001, a PP-based granulate produced by Nanocyl, containing 20 w/w%. The application of the reinforcing phase is justified by the fact that, compared to glass fibre, it deteriorates the life cycle of the tool much less, and it can exert its effect with a smaller weight ratio.

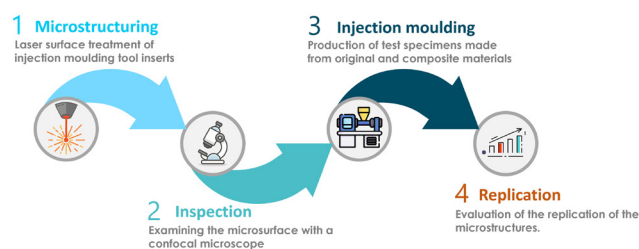


Fig. 1 Steps of the research process in infographic

From the results of differential scanning calorimetry (DSC) measurements, it can be concluded that the crystallization temperatures of PP/CNT composites and the recycled varied between 162–164 °C. The effect of CNT caused a minimal increase in the melting temperature. The crystalline fractions of PP/CNT composites are 8–10% higher than that of the pure PP matrix. The initial crystallization temperatures of PP/CNT composites and their recycled versions showed an increase of 6–8 °C, and 8–10 °C in the peak crystallization temperature compared to the neat PP material depending on the CNT content.

2.2 Methods

Following the selection of the matrix and the reinforcing phase, the nanocomposite was produced. To ensure proper homogenization, the mixing process was conducted using a Labtech Scientific twin screw extruder in two steps. Two mixtures were prepared containing 0.1 w/w% and 0.5 w/w% CNT. In the automotive industry and the present research, the effect of recycling is an important aspect, so the mixtures were first used to produce test specimens, which were then ground and reprocessed.

This process was repeated five times to obtain recycled nanocomposites containing 0.1 w/w% and 0.5 w/w% CNTs subjected to thermomechanical stress [27, 30].

The melt flow index (MFI) was measured using an Instron CEAST MF20 modular flow index meter at 190, 210 and 230 °C with a load of 2.16 kg. The height of the ribs measured on the test specimens was measured in 3 sections, and 3 measurements were taken in each section:

- 10 mm from the starting point of the structures,
- in the middle of the structured section and
- 10 mm from the end of the structured section.

The surface structure (micro-ribs) on the tool insert was created using a Coherent Monaco 1035-80-40 femtosecond laser. Although the focus of the research was not the optimization of the surface treatment with the laser, the machining speed of the technology and the quality of the surface created were important for industrial applicability [31]. The optimal settings for laser structuring after surface treatment tests are shown in Table 1. The size of the structured surface was 78 × 10 mm. Digital models of the designed injection moulding insert (Fig. 2(a)) and its product (Fig. 2(b)) are shown in Fig. 2.

The 3D topologies of the surface structures were analyzed using an Olympus LEXT5100 confocal microscope.

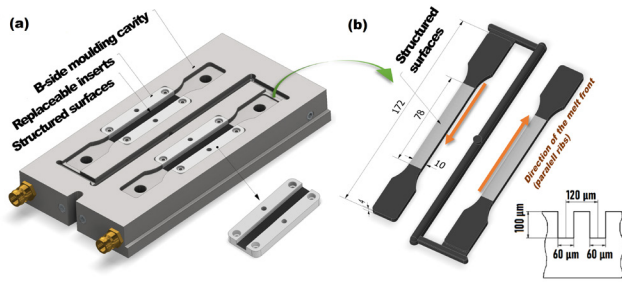


Fig. 2 Microstructured insert (a) and the moulded product (b)

Table 1 The technical parameters of the femtosecond laser

Applied technical specification	
Average power	24 W (40%)
Energy	32 μJ (on 750 kHz)
Frequency	750 kHz
Wave length	1035 ± 5 nm
Pulse length	277 fs
Mode	TEM ₀₀ , (M ² < 1.2)
Scanning speed	0.5 m/s

The accuracy of the instrument in the Z direction is $0.15 \mu\text{m} + L/100$, where L is the length of the measured section. The measurement accuracy in the Z direction is therefore $0.79 \mu\text{m}$ for $64 \mu\text{m}$ long sections. The resolution in the X-Y direction is 1 nm . For all three directions, the repeatability with the objective used is $0.03 \mu\text{m}$. The depth of the structured surfaces was only $\pm 5 \mu\text{m}$ compared to the planned $100 \mu\text{m}$. The 3D topology (Fig. 3(a)) was created in Gwyddion software.

A Gaussian filter was employed to mitigate measurement noise, without impacting the average of the measured values. The confocal microscope measurements were used to generate the surface profile of the inserts shown in Fig. 3(b). The measurements were performed

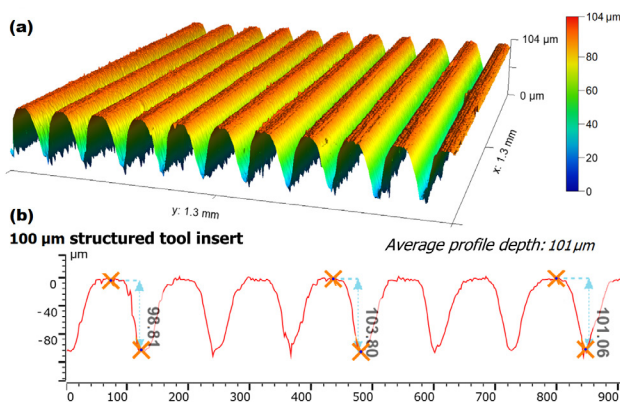


Fig. 3 3D topological image of the laser surface-treated moulding insert (a) and a cross-sectional profile of the microstructured insert (b)

on three sections per experimental specimen, with three groove depths. Although the manufactured groove depths were within $\pm 5 \mu\text{m}$ of the design, the rest material was generated from the laser beam intensity distribution.

The micro-geometrical features and the structure profiles shown in Fig. 3(a) were influenced by the laser source. The shape of the intensity distribution can be observed in the cross-section of the surface-treated cavity. The laser beam is in TEM₀₀ mode, and the beam intensity distribution follows a Gaussian distribution as shown in Fig. 4(b).

After the injection moulding, the insert was structured and inspected, and polymer specimens were manufactured. The tool was equipped with a special sensor technology, which allowed a stable range of injection rates to be measured. During the test, the viscosity could be determined by continuously increasing the injection rate and measuring cavity and injection pressure. In the stable range, where viscosity no longer decreases significantly, the injection rate was $90 \text{ cm}^3/\text{s}$, so this value was recorded as a constant in the series of experiments. Other constants were the mould temperature of $40 \text{ }^\circ\text{C}$ and the cooling time of 40 s . Since the determination of the melt temperature was also recorded in a range ($190\text{--}230 \text{ }^\circ\text{C}$), it was also included as a three-level variable in the experiment. The backpressure value was also tested as a variable at three levels, creating a two-factor three-level experimental design (Table 2).

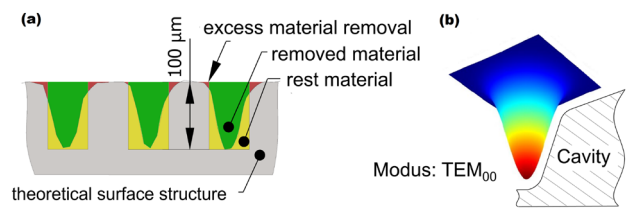


Fig. 4 Geometric features of the laser-formed moulding tool (a) and the intensity of the laser beam used (b)

Table 2 Experimental design used to produce moulded specimens

Experiment	Melt temperature [$^\circ\text{C}$]	Backpressure [bar]
1.	190	200
2.	190	500
3.	190	800
4.	210	200
5.	210	500
6.	210	800
7.	230	200
8.	230	500
9.	230	800

The test specimens were injection moulded on a Wittmann Battenfeld Ecopower 55 injection moulding machine. The moulding quality of the moulding inserts can be assessed by using the TR-factor according to the literature. The higher the TR-factor, the better the replication. In this case, the greater the rib height formed on the polymer product and the closer to the depth of the structure on the insert, the closer the value of the TR-factor is to 1 [32].

3 Results and discussion

When combined with PP, the carbon nanotubes can form a physical cross-linking mesh, thus inhibiting the mobility of the molecules. As the ratio of the reinforcing material increases, the MFI decreases, which may lead to a deterioration of the filling quality. At the same time, recyclization in PP/CNT nanocomposite leads to chain degradation [9, 14, 16]. Therefore, the viscosity of the original (base) material decreases, the MFI value increases, so better filling, i.e. more accurate mapping of surface patterns, can be expected. Due to these two opposing effects, the MFI of the raw materials was determined at the temperatures used (Fig. 5) before evaluating the TR-factor results.

The MFI value of the original material according to the data sheet at 230 °C is 6.5 g/10 min, confirmed by the measurements. The viscosity decreases with increasing temperature. At a lower CNT content of 0.1 w/w%, the melt flow index at 210 °C is almost the same as that of the original base material.

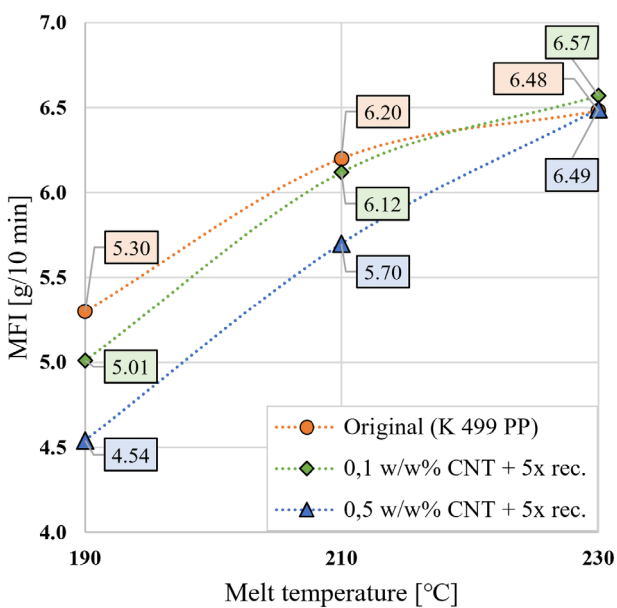


Fig. 5 The MFI values of the original PP raw material and its recycled and CNT reinforced composites at the examined melt temperatures

The Taguchi experimental design calculates signal-to-noise ratios (SN) that can filter out the increase or decrease in variance caused by the average. The shape of the SN used depends on the nature of the qualitative characteristic. Based on the experimental design, a main effect diagram (Fig. 6) can be generated in Minitab software to determine how process parameters and surface structures affect the replication (TR-factor). The evaluation aimed to determine the influence of certain factors on microstructure replication and variance. Since the aim was to improve the fill-in as a quality aspect, the "Larger is Better" Eq. (1) was used for the evaluation.

$$SN_L = -10 \log \left(\frac{\sum_i \left(\frac{1}{y_i^2} \right) / n}{n} \right), \quad (1)$$

where:

- y : value measured in an experimental setting,
- n : number of measured values.

The main effect analysis of the 100 µm structure depth tool insert showed that the melt temperature was significant for the filling, and the TR-factor was mainly influenced by this process parameter. By increasing the melt temperature, the filling improved. The enhancement of backpressure had a similar positive effect on the deposition, but the magnitude of the influence was approximately half [32].

It is observed that the TR-factor is lower for products made from carbon nanotube-reinforced base material using the same technology, and the filling rate decreases with increasing ratio of the reinforcing phase. This is confirmed by the Delta values illustrated in Table 3.

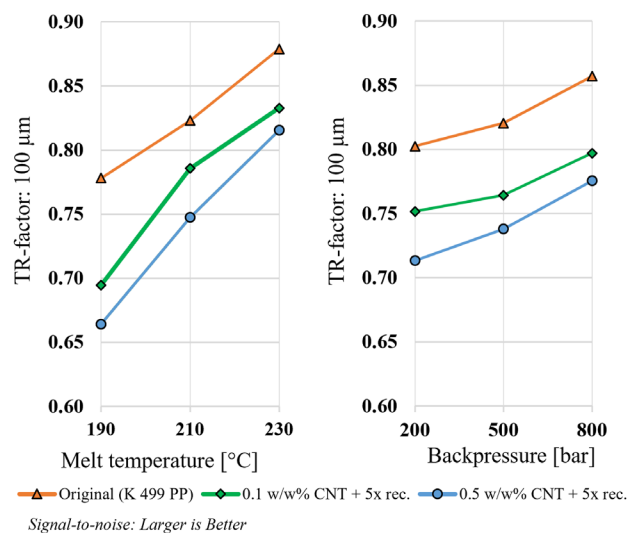


Fig. 6 Filling of the 100 µm deep cavity structures: main effects of process parameters

Table 3 Ranking of factors influencing the TR-factor

Original (K 499 PP)		
Level	Melt temperature	Backpressure
1	0.778	0.803
2	0.823	0.821
3	0.879	0.857
Delta	0.101	0.055
Rank	1	2
0.1 w/w% CNT + 5x rec.		
Level	Melt temperature	Backpressure
1	0.695	0.752
2	0.786	0.764
3	0.833	0.797
Delta	0.138	0.045
Rank	1	2
0.5 w/w% CNT + 5x rec.		
Level	Melt temperature	Backpressure
1	0.664	0.713
2	0.747	0.738
3	0.815	0.776
Delta	0.151	0.062
Rank	1	2

Based on the main effects plot (Fig. 6), a combination of appropriate manufacturing parameters can result in improved infill in favour of nanocomposite test specimens manufactured from recycled raw material compared to the original raw material. Fig. 6 also shows that the recycling and reinforcing phases deteriorated the filling. The shift in the lines of influence varies with the CNT content but not with its percentage.

It can be concluded that for the replication of structures with a depth of 100 μm , the filling was influenced differently by CNT content and recycling. 3D topological images were also taken of the pattern formed on the surface of the moulded products (Fig. 7) so that the filling is more clearly visible. The replication of the specimen manufactured with the highest variable parameters above 80% is observed, as well as the uniform shape tracking of the micro geometries.

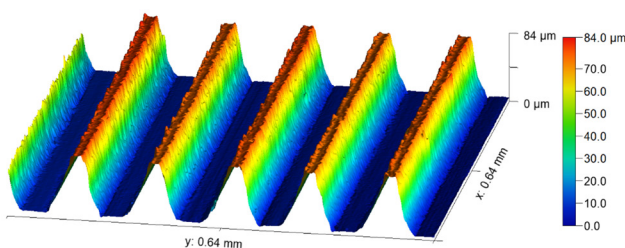


Fig. 7 3D topology of a PP product with 0.5 w/w% CNT content replicated the 100 μm deep cavity structures, produced according to experiment number 9

The data measured on the confocal microscope profiles were used to plot the TR-factor values of the microstructures with the three material types. The results are plotted on a 3D surface within the range of variables investigated in Fig. 7, which shows that both the increase in the melt temperature and the increase in the back-pressure values have a positive effect on the filling. The TR-factor is more affected by the melt temperature, which can be observed from the formation of the surfaces.

Based on the results, a technological and industrial recommendation for the evolution of the replication (TR-factor) was made using a mathematical model. Analysis of variance (ANOVA) was used to evaluate the experimental data for quality variables. The response surfaces (Fig. 8) are suitable to provide a solution to the objective function by specifying the technological variables. When applied, the zone of expected values can be selected by linking the chosen values of the technology settings on the vertical and horizontal axes. To solve the regression equations, it was necessary to code the process parameters of different magnitudes into units between -1 and $+1$ using Minitab software. In that way, the interactions could be compared.

Fig. 8 illustrates that the increase in the examined factors corresponds to the filling rate with the recycled carbon nanotube-reinforced materials, reaching parity with the filling rate of the original material.

Elevating the melt temperature to 230 $^{\circ}\text{C}$ (at 800 bar backpressure) resulted in better filling of the ribs. The material with a carbon nanotube content of 0.1 w/w% shows an average reduction of 5% compared to the original material. Similarly, at a 0.5 w/w% carbon nanotube content, the height of the micro-ribs displayed an average reduction of 7%. Inference can be drawn that the adverse impact of the reinforcing phase on filling can be compensated by increasing the melt temperature.

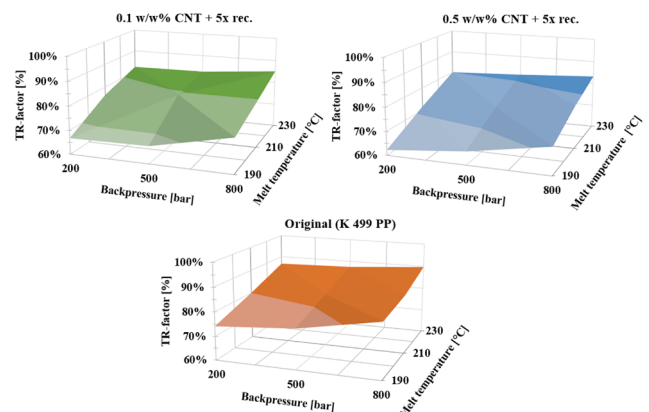


Fig. 8 Filling of microstructures as a function of backpressure and melt temperature

4 Conclusions

It has been found in various papers [30–32] that functional microstructures are created to increase mechanical properties. In injection moulding, the effect of micro-ribs on the melt front can lead to structural modifications of the material. Even the closed-loop recycled polymers will lose strength, despite the specifications on the datasheet. Recycling reduces the molecular weight of the polymer raw material, and its distribution and degrades the length of the molecular chains. These cause a negative effect in terms of mechanical properties, but the broken molecular chain leads to a decrease in viscosity. This phenomenon can be compensated by reinforcing phases, but at the same time, the filling quality of the micro-structures is reduced. Sustainability can be ensured using an expensive reinforcing phase at a low ratio. The viscosity of the recycled nanocomposite was negatively affected by the reinforcing phase content. The replication of the microstructures in the mould cavity was

further reduced by increasing the ratio of the reinforcing agent. The processing parameters significantly influenced the value of TR-factors, which provide information on the quality of the infill. By increasing the melt temperature and the backpressure, the quality of replication can be enhanced.

However, it is not only dependent on the technological parameters and the number of reinforcing phases, but also on the number of recycling cycles and the geometry of the moulded parts. The research results suggest that, thanks to controlled, sensor-monitored conditions and appropriate processing parameters, the replication quality of microfibrils in nanocomposite products can be equivalent to that of the original materials. This will bring significant industrial benefits by enabling the production of sustainable and high-quality products at lower cost and with less environmental impact. The research results may offer valuable insights to enhance the quality of the filling procedure.

References

- [1] Bulk Chemicals "Automotive Plastics Market Size, Share & Trends Analysis Report", 2021. [online] Available at: <https://www.grandviewresearch.com/industry-analysis/automotive-plastics-market> [Accessed: 06 May 2024]
- [2] ASTM "ASTM D883-19 Standard Terminology Relating to Plastics", ASTM International - Standards Worldwide, West Conshohocken, PA, USA, 2019. [online] Available at: <https://www.astm.org/d0883-22.html> [Accessed: 06 May 2024]
- [3] ISO "ISO 4618:203(en) Paints and varnishes - Terms and definitions", International Organization for Standardization, Geneva, Switzerland, 2023. [online] Available at: <https://www.iso.org/standard/81386.html> [Accessed: 06 May 2024]
- [4] Sha, B., Dimov, S., Griffiths, C., Packianather, M. S. "Investigation of micro-injection moulding: Factors affecting the replication quality", *Journal of Materials Processing Technology*, 183(2–3), pp. 284–296, 2007. <https://doi.org/10.1016/j.jmatprotec.2006.10.019>
- [5] Piccolo, L., Sorgato, M., Batal, A., Dimov, S., Lucchetta, G., Masato, D. "Functionalization of Plastic Parts by Replication of Variable Pitch Laser-Induced Periodic Surface Structures", *Micromachines*, 11(4), 429, 2020. <https://doi.org/10.3390/mi11040429>
- [6] Arzt, E., Quan, H., McMeeking, R. M., Hensel, R. "Functional surface microstructures inspired by nature – From adhesion and wetting principles to sustainable new devices", *Progress in Material Science*, 120, 100823, 2021. <https://doi.org/10.1016/j.pmatsci.2021.100823>
- [7] Li, J., Ma, H., Liu, W., Jiang, S., Pan, B. "Effects of Cavity Thickness and Mold Surface Roughness on the Polymer Flow during Micro Injection Molding", *Polymers*, 15(2), 326, 2023. <https://doi.org/10.3390/polym15020326>
- [8] Theilade, U. A., Hansen, H. N. "Surface microstructure replication in injection molding", *The International Journal of Advanced Manufacturing Technology*, 33(1–2), pp. 157–166, 2007. <https://doi.org/10.1007/s00170-006-0732-y>
- [9] Zhang, J., Panwar, A., Bello, D., Jozokos, T., Isaacs, J. A., Barry, C., Mead, J. "The effects of recycling on the properties of carbon nanotube-filled polypropylene composites and worker exposures", *Environmental Science: Nano*, 3(2), pp. 409–417, 2016. <https://doi.org/10.1039/C5EN00253B>
- [10] Attia, U. M., Alcock, J. R. "An evaluation of process-parameter and part-geometry effects on the quality of filling in micro-injection moulding", *Microsystem Technologies*, 15,(12), pp. 1861–1872, 2009. <https://doi.org/10.1007/s00542-009-0923-1>
- [11] Ádám, B., Weltsch, Z. "Thermal and Mechanical Assessment of PLA-SEBS and PLA-SEBS-CNT Biopolymer Blends for 3D Printing", *Applied Sciences*, 11(13), 6218, 2021. <https://doi.org/10.3390/app11136218>
- [12] Li, J., Ma, H., Liu, W., Jiang, S., Pan, B. "Effects of cavity thickness and mold surface roughness on the polymer flow during micro injection molding", *Polymers*, 15(2), 326, 2023. <https://doi.org/10.3390/polym15020326>
- [13] Wang, G., Zhao, G., Wang, X. "Effects of cavity surface temperature on reinforced plastic part surface appearance in rapid heat cycle moulding", *Materials & Design*, 44, pp. 509–520, 2013. <https://doi.org/10.1016/j.matdes.2012.08.039>
- [14] Zdiri, K., Elamri, A., Hamdaoui, M., Harzallah, O., Khenoussi, N., Brendlé, J. "Reinforcement of recycled PP polymers by nanoparticles incorporation", *Green Chemistry Letters and Reviews*, 11(3), pp. 296–311, 2018. <https://doi.org/10.1080/17518253.2018.1491645>

- [15] Bata, A., Toth, G., Nagy, D., Belina, K. "Melt shear viscosity of original and recycled PET in wide range shear rate", *Journal of Physics: Conference Series*, 1045(1), 012007, 2018.
<https://doi.org/10.1088/1742-6596/1045/1/012007>
- [16] Gim, J., Han, E., Rhee, B., Friesenbichler, W., Gruber, D. P. "Causes of the Gloss Transition Defect on High-Gloss Injection-Molded Surfaces", *Polymers*, 12(9), 2100, 2020.
<https://doi.org/10.3390/polym12092100>
- [17] Masato, D., Sorgato, M., Lucchetta, G. "Analysis of the influence of part thickness on the replication of micro-structured surfaces by injection molding", *Materials & Design*, 95, pp. 219–224, 2016.
<https://doi.org/10.1016/j.matdes.2016.01.115>
- [18] Regi, F., Guerrier, P., Zhang, Y., Tosello, G. "Experimental characterization and simulation of thermoplastic polymer flow hesitation in thin-wall injection molding using direct in-mold visualization technique", *Micromachines*, 11(4), 428, 2020.
<https://doi.org/10.3390/mi11040428>
- [19] Kun, K., Weltsch, Z. "Effect of Femtosecond-Laser-Structured Injection Molding Tool on Mechanical Properties of the Manufactured Product", *Polymers*, 13(13), 2187, 2021.
<https://doi.org/10.3390/polym13132187>
- [20] Modica, F., Basile, V., Surace, R., Fassi, I. "Replication Study of Molded Micro-Textured Samples Made of Ultra-High Molecular Weight Polyethylene for Medical Applications", *Micromachines*, 14(3), 523, 2023.
<https://doi.org/10.3390/mi14030523>
- [21] Bagalkot, A., Pons, D., Symons, D., Clucas, D. "The Effects of Cooling and Shrinkage on the Life of Polymer 3D Printed Injection Moulds", *Polymers*, 14(3), 520, 2022.
<https://doi.org/10.3390/polym14030520>
- [22] van Assenbergh, P., Meinders, E., Geraedts, J., Dodou, D. "Nanostructure and Microstructure Fabrication: From Desired Properties to Suitable Processes", *Small*, 14(20), 1703401, 2018.
<https://doi.org/10.1002/smll.201703401>
- [23] Attia, U. M., Marson, S., Alcock, J. R. "Micro-injection moulding of polymer microfluidic devices", *Microfluid and Nanofluidics*, 7(1), pp. 1–28, 2009.
<https://doi.org/10.1007/s10404-009-0421-x>
- [24] Gim, J., Turng, L. S. "A review of current advancements in high surface quality injection molding: Measurement, influencing factors, prediction, and control", *Polymer Testing*, 115, 107718, 2022.
<https://doi.org/10.1016/j.polymertesting.2022.107718>
- [25] Trotta, G., Vázquez, R. M., Volpe, A., Modica, F., Ancona, A., Fassi, I., Osellame, R. "Disposable Optical Stretcher Fabricated by Microinjection Moulding", *Micromachines*, 9(8), 388, 2018.
<https://doi.org/10.3390/mi9080388>
- [26] Lendvai, L., Ronkay, F., Wang, G., Zhang, S., Guo, S., Ahlawat, V., Singh, T. "Development and characterization of composites produced from recycled polyethylene terephthalate and waste marble dust", *Polymer Composites*, 43(6), pp. 3951–3959, 2022.
<https://doi.org/10.1002/pc.26669>
- [27] Chen, D., Wang, Y., Zhou, H., Huang, Z., Zhang, Y., Guo, C. F., Zhou, H. "Current and future trends for polymer micro/nanoprocessing in industrial applications", *Advanced Materials*, 34(52), 2200903, 2022.
<https://doi.org/10.1002/adma.202200903>
- [28] Nagy, D., Belina, K. "Measuring viscosity of polyethylene blends using a rotational rheometer", *Journal of Physics: Conference Series*, 1045(1), 012030, 2018.
<https://doi.org/10.1088/1742-6596/1045/1/012030>
- [29] Raimbault, O., Benayoun, S., Anselme, K., Mauclair, C., Bourgade, T., Kietzig, A.-M., Girard-Lauriault, P.-L., Valette, S., Donnet, C. "The effects of femtosecond laser-textured Ti-6Al-4V on wettability and cell response", *Materials Science and Engineering: C*, 69, pp. 311–320, 2016.
<https://doi.org/10.1016/j.msec.2016.06.072>
- [30] Lee, J. H., Park, S. H., Kim, S. H., Ito, H. "Replication and surface properties of micro injection molded PLA/MWCNT nanocomposites", *Polymer Testing*, 83, 106321, 2020.
<https://doi.org/10.1016/j.polymertesting.2019.106321>
- [31] Preußner, J., Oeser, S., Pfeiffer, W., Temmler, A., Willenborg, E. "Microstructure and Residual Stresses of Laser Structured Surfaces", *Advanced Materials Research*, 996, pp. 568–573, 2014.
<https://doi.org/10.4028/www.scientific.net/AMR.996.568>
- [32] Yokoi, H., Han, X., Takahashi, T., Kim, W. K. "Effects of molding conditions on transcription molding of microscale prism patterns using ultra-high-speed injection molding", *Polymer Engineering and Science*, 46(9), 11401146, 2006.
<https://doi.org/10.1002/pen.20519>